Fusion of Bayesian Maximum Entropy Spectral Estimation and Variational Analysis Methods for Enhanced Radar Imaging

Yuriy Shkvarko[1], Rene Vazquez-Bautista[1], and Ivan Villalon-Turrubiates[1]

[1] CINVESTAV Jalisco, Avenida Científica 1145, Colonia El Bajío, 45010,
Telephone (+52 33) 3770-3700, Fax (+52 33) 3770-3709, Zapopan Jalisco, México
{shkvarko, fvazquez, villalon}@gdl.cinvestav.mx
http://www.gdl.cinvestav.mx

Abstract. A new fused Bayesian maximum entropy–variational analysis (BMEVA) method for enhanced radar/synthetic aperture radar (SAR) imaging is addressed as required for high-resolution remote sensing (RS) imagery. The variational analysis (VA) paradigm is adapted via incorporating the image gradient flow norm preservation into the overall reconstruction problem to control the geometrical properties of the desired solution. The metrics structure in the corresponding image representation and solution spaces is adjusted to incorporate the VA image formalism and RS model-level considerations; in particular, system calibration data and total image gradient flow power constraints. The BMEVA method aggregates the image model and system-level considerations into the fused SSP reconstruction strategy providing a regularized balance between the noise suppression and gained spatial resolution with the VA-controlled geometrical properties of the resulting solution. The efficiency of the developed enhanced radar imaging approach is illustrated through the numerical simulations with the real-world SAR imagery.

1 Introduction

The Bayesian approach for high resolution radar image formation is detailed in many works; here we refer to [1] – [3] where such approach is adapted to remote sensing (RS) applications considered in this paper. Further information theoretic-based development of the Bayesian imaging paradigm that employs the maximum entropy (ME) robust regularization of the nonlinear image reconstruction inverse problem was developed recently in [4] – [6] where it was addressed to as the Bayesian maximum entropy (BME) method. On the other hand, an alternative approach to image enhancement and noise suppression was proposed and detailed in [7] – [10] where the variational analysis (VA) paradigm was employed to incorporate a priori information regarding the image geometrical properties

specified by its gradient flow over the image frame, while no particular model of the imaging system was employed. In view of this, the VA paradigm may be classified as system model-free image enhancement approach [7]-[10]. Some second order partial differential equation (PDE) models for specifying the gradient flow over the image frame were employed in different VA approaches to incorporate the intrinsic image geometry properties into the enhancement procedures [7] – [10]. On one hand, a considerable advantage of the VA paradigm relates to its flexibility in designing the desirable error metrics in the corresponding image representation and reconstruction spaces via defining different variational cost functionals and relevant PDE in the overall VA optimization problem [8], [10]. On the other hand, the crucial limitation of all VA-based methods lies in their descriptive system-model-free deterministic regularization nature because these methods do not employ statistical optimization strategies, i.e. do not consider a particular RS system model, and do not incorporate image and noise statistics into the VA enhancement strategy. In contrast, the BME approach is based on the statistical optimization paradigm [4], [5], [11] adapted for a particular RS system model and robust a priori information about the statistics of noise and the desired image. The latter is associated with the spatial spectrum pattern (SSP) of the wavefield backscattered from the probing surface. As the SSP represents the power distribution in the RS environment, the power non-negativity constraint is incorporated implicitly in the BME strategy but that do not incorporate specific VA geometrical properties of the image, e.g. its gradient flow over the scene/frame. In view of this, the following problem arises: how to aggregate the statistically optimal BME method with the VA formalism for enhanced RS imaging that incorporate the advantages of both the VA and the BME approaches? An approximation to this problem was initially proposed in [12] where it was considered in the context of alleviating the ill-posed nature of the VA techniques that employ the anisotropic diffusion RDE as an optimization criterion [7], [8]. In this paper, we address a new balanced statistical-regularization fusion paradigm that leads to a new method addressed to as the fused Bayesian maximum entropy variational analysis (BMEVA) technique. The VA paradigm is adapted via incorporating the image gradient norm preservation into the overall reconstruction problem to control the geometrical properties of the desired solution.

2 Problem Statement

Following [1], [3], [4] we define the model of the observation wavefield u by specifying the stochastic equation of observation (EO) of an operator form

$$u=Se+n;\ \ e\in \mathrm{E};\ \ u,n\in \mathrm{U};\ \ S\!:\mathrm{E}\rightarrow\mathrm{U}, \qquad (\mathbf{1})$$

in Hilbert signal spaces E and U with the metrics structures induced by the inner products, $[u_1,u_2]_{\mathrm{U}}$ and $[e_1,e_2]_{\mathrm{E}}$, respectively, where the Gaussian zero-mean random fields e, n, and u correspond to the initial coherent backscattered field, noise and

observed wavefield, respectively. Next, taking into account the experiment design (ED) theory-based projection formalism [4], [5] we proceed from the operator form EO (1) to its conventional finite-dimensional vector form,

$$\mathbf{U}=\mathbf{SE}+\mathbf{N}\ , \qquad (\mathbf{2})$$

where **E**, **N** and **U** define the zero-mean vectors composed of the coefficients E_k , N_m , and U_m of the numerical approximations (sample decomposition [4]) of the relevant operator-form EO (1), i.e. **E** represents the K-D vector composed with the coefficients $\{E_k=[e,g_k]_{\mathrm{E}},\ k=1,\ldots,K\}$ of the K-D approximation, $e_{(K)}(\mathbf{r})=(P_{\mathrm{E}(K)}e)(\mathbf{r})=\sum E_k g_k(\mathbf{r})$, of the initial backscattered wavefield $e(\mathbf{r})$ distributed over the RS scene (image frame) $R\ni\mathbf{r}$ [4], and $P_{\mathrm{E}(K)}$ is a projector onto the K-D signal approximation subspace $\mathrm{E}_{(K)}=P_{\mathrm{E}(K)}\mathrm{E}=\mathrm{Span}\{g_k\}$ spanned by some properly chosen set of K basis functions $\{g_k(\mathbf{r})\}$ [5], [11]. The M-by-K matrix **S** that approximates the signal formation operator (SFO) in (2) is given now by [4]

$$S_{mk}=[Sg_k,\varphi_m]_{\mathrm{U}};\ m=1,\ldots,M;\ k=1,\ldots,K\ , \qquad (\mathbf{3})$$

where the set of the base functions $\{\varphi_m(\mathbf{y})\}$ that span the finite-dimensional spatial observation subspace $\mathrm{U}_{(M)}=P_{\mathrm{U}(M)}\mathrm{U}=\mathrm{Span}\{\varphi_m\}$ defines the corresponding projector $P_{\mathrm{U}(M)}$ induced by these array spatial response characteristics $\{\varphi_m(\mathbf{y})\}$ [11].

The ED aspects of the SSP estimation inverse problem involving the analysis of how to choose (finely adjust) the basis functions $\{g_k(\mathbf{r})\}$ that span the signal representation subspace $\mathrm{E}_{(K)}=P_{\mathrm{E}(K)}\mathrm{E}=\mathrm{Span}\{g_k\}$ for a given observation subspace $\mathrm{U}_{(M)}=\mathrm{Span}\{\varphi_m\}$ were investigated in more details in the previous studies [5], [14]. Here, we employ the pixel-format basis [5], [11] and the ED considerations regarding the metrics structure in the solution space defined by the inner product

$$\|\mathbf{B}\|^2_{\mathrm{B}(K)}=[\mathbf{B},\mathbf{MB}]\ , \qquad (\mathbf{4})$$

where matrix **M** is referred to as the metrics inducing operator [4], [5]. Hence, the selection of **M** provides additional geometrical degrees of freedom of the problem model. In this study, we incorporate the model of **M** that corresponds to a matrix-form approximation of the Tikhonov's stabilizer of the second order that was numerically designed in [4].

The RS imaging problem under consideration is to find an BMEVA-optimal estimate $\hat{B}(\mathbf{r})$ of the SSP $B(\mathbf{r})$ distributed over the scene (image frame) $R\ni\mathbf{r}$ by processing whatever values of the discrete measurements **U** of the data signals (2) are available that incorporates also non-trivial image model information into the estimation strategy. Thus, the purpose of our study is to develop a generalization of the BME estimator [4], [5] adapted for the high-resolution SSP reconstruction problem that aggregates the prior image model considerations induced by the adopted metrics structure (4) in the image representation and solution spaces with geometrical considerations invoked from the VA formalism [7], [10].

3 Generalized BME Estimator for SSP

The objective of a statistical BME estimator is to obtain a unique and stable estimate $\hat{\mathbf{B}}$ by processing the measurement data $\mathbf{U}$ in an optimum fashion, "optimum" being considered in a sense of the Bayes minimum risk strategy [4], [13]. Note that the ill-posed nature of such inverse problem results in the ill-conditioned SFO [3], [11]. The ME principle [13] provides the well-grounded way to alleviate the problem ill-poseness. According to the ME paradigm [13], the whole image is viewed as a composition of a great amount of elementary discrete speckles (pixels) with the elementary "pixel brightness" normalized to the elementary unit of the adopted image representation scale, e.g. 256 grades of gray in the conventional gray-scale image formats [6], [11]. Following the ME approach developed in [4], the a priori probability density function (pdf) $p(\mathbf{B})$ of the discrete-form image $\mathbf{B}$ is to be defined via maximization of the entropy of the image probability that satisfies also the constraints imposed by the prior knowledge [5]. The vector $\mathbf{B}$ is viewed as an element of the nonnegative set B_C of the K-D vector space $\mathrm{B}_C \ni \mathbf{B}$ with the squared norm induced by the inner product (4). In addition, the physical factors of the experiment can be generalized via imposing the physically obvious ED constraint that bounds the average squared norm of the SSP by some preserved constant total power E_0, i.e.

$$\int_{\mathbf{B}_C} [\mathbf{B}, \mathbf{M}\mathbf{B}] p(\mathbf{B}) d\mathbf{B} = E_0 \ , \tag{5}$$

which specifies the calibration constraint for the SSP reconstruction. Thus, the a priori pdf $p(\mathbf{B})$ is to be found as a solution to the Lagrange entropy maximization problem with the Lagrange multipliers α, and λ and is specified as follows [4]

$$\begin{aligned} -\int_{\mathbf{B}_C} \ln p(\mathbf{B}) p(\mathbf{B}) d\mathbf{B} - \alpha\Big(\int_{\mathbf{B}_C} [\mathbf{B}, \mathbf{M}\mathbf{B}] p(\mathbf{B}) d\mathbf{B} - E_0\Big) \\ - \lambda\Big(\int_{\mathbf{B}_C} p(\mathbf{B}) d\mathbf{B} - 1\Big) \to \max_{p(\mathbf{B})} \ , \end{aligned} \tag{6}$$

for $\mathbf{B} \in B_C$, and $p(\mathbf{B})=0$ otherwise. Routinely following the variational scheme detailed in [4] we obtain the solution to (6) that yields the Gibbs-type a priori pdf

$$p(\mathbf{B} \mid \alpha) = \exp\{-\ln \sum(\alpha) - \alpha[\mathbf{B}, \mathbf{M}\mathbf{B}]\} \ , \tag{7}$$

where $\sum(\alpha)$ represents the so-called Boltzmann statistical sum [4], in which the normalization parameter α must be adjusted to satisfy the calibration constraint (5).

Next, we define the log-likelihood function of the desired vector $\mathbf{B}$ [4] given the Gaussian measurements $\mathbf{U}$ specified by the EO (2)

$$\begin{aligned} \Lambda(\mathbf{B} \mid \mathbf{U}) = \ln p(\mathbf{B} \mid \mathbf{U}) = -\ln \det\{\mathbf{S}\mathbf{D}(\mathbf{B})\mathbf{S}^{+} + \mathbf{R}_{\mathbf{N}}\} \\ - [\mathbf{U}, (\mathbf{S}\mathbf{D}(\mathbf{B})\mathbf{S}^{+} + \mathbf{R}_{\mathbf{N}})^{-1}\mathbf{U}]. \end{aligned} \tag{8}$$

Using (7) and (8), the BME strategy for SSP reconstruction can be stated now as the following nonlinear optimization problem [15]

$$\hat{\mathbf{B}} = \arg\min_{\mathbf{B},\alpha}\{-\Lambda(\mathbf{B} \mid \mathbf{U}) - \ln p(\mathbf{B} \mid \alpha)\} \ . \tag{9}$$

The optimization problem (9) is structurally similar to one considered in [4]. The modifications incorporated in this particular study include the redefined metrics structure (4) and boundary constraint (6). Thus, following the approach developed in [4], the desired solution to (9) in a form of the nonlinear procedure is

$$\hat{\mathbf{B}} = \mathbf{W}(\hat{\mathbf{B}})[\mathbf{V}(\hat{\mathbf{B}}) - \mathbf{Z}(\hat{\mathbf{B}})] \ . \tag{10}$$

Here, $\mathbf{V}(\hat{\mathbf{B}}) = \{\mathbf{F}(\hat{\mathbf{B}})\mathbf{U}\mathbf{U}^{+}\mathbf{F}^{+}(\hat{\mathbf{B}})\}_{\text{diag}}$ represents a vector that has a statistical meaning of a sufficient statistics (SS) for the SSP estimator, operator $\mathbf{F}(\hat{\mathbf{B}}) = \mathbf{D}(\hat{\mathbf{B}})(\mathbf{I} + \mathbf{S}^{+}\mathbf{R}_{\mathbf{N}}^{-1}\mathbf{S}\mathbf{D}^{-1}(\hat{\mathbf{B}}))^{-1}\mathbf{S}^{+}\mathbf{R}_{\mathbf{N}}^{-1}$ is referred to as the SS formation operator, the vector $\mathbf{Z}(\hat{\mathbf{B}}) = \{\mathbf{F}(\hat{\mathbf{B}})\mathbf{R}_{\mathbf{N}}\mathbf{F}^{+}(\hat{\mathbf{B}})\}_{\text{diag}}$ represents the shift (bias) vector, and $\mathbf{W}(\hat{\mathbf{B}}) = (\mathbf{T}(\hat{\mathbf{B}}) + 2\alpha\mathbf{D}^{2}(\hat{\mathbf{B}})\mathbf{M})^{-1}$ has the statistical meaning of a solution dependent (i.e., adaptive) regularizing window operator with the stabilizer $\mathbf{T}(\hat{\mathbf{B}}) = \text{diag}\{\{\mathbf{S}^{+}\mathbf{F}^{+}(\hat{\mathbf{B}})\mathbf{F}(\hat{\mathbf{B}})\mathbf{S}\}_{\text{diag}}\}$. Adaptation is to be performed over both the current SSP estimate, $\hat{\mathbf{B}}$, and the normalization constant α adjusted to satisfy the calibration constraint (5).

4 VA Formalism for SSP Enhancement

The goal of adapting the VA formalism is to enhance the overall quality of the SSP reconstructed via the BMEVA procedure (10). The VA purpose is to perform the simultaneous extraction and synthesis of the geometrical image model information from a sequence of the evolutionary innovated image reconstructions (the *frames* in the VA terminology [10]) via incorporating the additional quality control functional (termed the *VA energy function*) into the overall BMEVA fusion strategy. The fusion process is dynamic with the fusion rate driven by some anisotropic diffusion gain function [7], [10] dictated by enhancement goals.

In our particular study, we limit ourselves with the control of the spatial gradient *flow* functional that results in the following VA energy minimization problem [10]

$$E_{VA}(B(\mathbf{r})) = \int_{R} \rho^{2}(|\nabla B(\mathbf{r})|, \mathbf{r}) d\mathbf{r} \to \min_{B(\mathbf{r})}, \tag{11}$$

where $\nabla = (\partial/\partial x \ \partial/\partial y)^{\mathrm{T}}$ defines the spatial differential operator [11] in the Cartesian coordinate system $\mathbf{r}=(x,y)^{\mathrm{T}} \in R$ that when applied to the SSP $B(\mathbf{r})$ returns

its gradient distribution $\nabla B(\mathbf{r})$ over the image frame R. Following the conventional definition for the VA energy function proposed in [7], [8] we adopt here the Lorentzian model of the error functional $\rho^2(\cdot)$ in (11), i.e.

$$\rho^2(\mathbf{r}) = \sigma^2 \log\left[1 + \frac{1}{2}\left(\frac{|\nabla B(\mathbf{r})|}{\sigma}\right)^2\right], \qquad (\mathbf{12})$$

which does not have an explicit dependence on the SSP $B(\mathbf{r})$, and where σ is a normalizing constant. With the Lorentzian error functional (12), the variational procedure $\delta E_{VA}(B(\mathbf{r})) = 0$ leads to the following Euler-Lagrange PDE as the VA optimization criterion [10]

$$\frac{\partial B(\mathbf{r},t)}{\partial t} = \nabla \cdot \left[\left(1 + \frac{|\nabla B(\mathbf{r},t)|^2}{2\sigma^2}\right)^{-1} \nabla B(\mathbf{r},t)\right], \qquad (\mathbf{13})$$

where t represents the *evolution* time translated into the iteration step number in the numerical reformulation of the PDE. The (13) defines the so-called Perona-Malik anisotropic diffusion equation [7]. It is a nonlinear PDE that has no analytic solution. Hence, the VA problem (11) can be solved only numerically employing some efficient iterative techniques [11], [12]. We next have to proceed with the fusion of the VA optimization problem (11) with the generalized BME strategy (9).

5 BMEVA Method and Numerical Implementation Technique

In the proposed BMEVA method, we aggregate the VA and BME approaches in the fused strategy

$$\hat{\mathbf{B}}_{BMEVA} = \arg\min_{\mathbf{B},\alpha|\gamma}\{-\Lambda(\mathbf{B}\,|\,\mathbf{U}) - \ln p(\mathbf{B}\,|\,\alpha) + \gamma \|\nabla \mathbf{B}\|_L^2\}, \qquad (\mathbf{14})$$

where $\nabla \mathbf{B}$ defines the numerical (pixel-format) approximation to the gradient vector, $\|\nabla \mathbf{B}\|_L^2$ represents the numerical approximation to the VA energy function (11) with the adopted Lorentzian error functional (12), and γ is referred to as the regularization parameter that balances the VA and BME criterions in the fused BMEVA strategy. In fact, the (14) is an NP-hard optimization problem [11], i.e. ill-posed in a computational sense [8], [11]. This problem has no analytic solution in polynomial time [8], hence, it must be solved numerically employing some practically reasonable regularization [11] to alleviate its ill-poseness. Here, we adopt the robust regularization approach based on the logarithm series tools [8]. Pursuing such technique, we first, substitute $\|\nabla \mathbf{B}\|_L^2$ in (14) by its second-order logarithm series approximation

$$|| \nabla \mathbf{B} ||_L^2 \approx \sigma^2 \sum_{n=1}^{2} \frac{(-1)^{n+1}}{n} \left(\frac{|| \nabla \mathbf{B} ||}{\sigma \sqrt{2}} \right)^{2n} = [\mathbf{B}, \mathbf{QB}] \ , \qquad (\mathbf{15})$$

where

$$\mathbf{Q} = (1/2)\mathbf{L} + \tau \mathbf{LL} \quad \text{and} \quad \tau = -1/8\sigma^2 \ , \qquad (\mathbf{16})$$

are the composed VA-regularized weighting matrix and the relaxation parameter, respectively, and the matrix $\mathbf{L}$ represents the numerical approximation [11] to the Laplacian second-order spatial differential operator ∇^2. With the approximations (15), (16) the strategy (14) can be transformed into

$$\hat{\mathbf{B}}_{BMEVA} = \arg\min_{\mathbf{B}, \alpha | \gamma} \{ -\Lambda(\mathbf{B} \mid \mathbf{U}) - \ln p(\mathbf{B} \mid \alpha) + \gamma [\mathbf{B}, \mathbf{QB}] \} \ . \qquad (\mathbf{17})$$

Due to the performed robust regularization, the modified strategy (17) relates now to a convex-type optimization problem [8], [11], thus, it can be solved numerically in a polynomial time [8]. The variational technique [4], [5] applied to the problem (17) yields the following numerical variational equation for the desired SSP

$$\mathbf{TB} + \mathbf{Z} - \mathbf{V} + 2\alpha \mathbf{D}^2 \mathbf{MB} + 2\gamma \mathbf{QB} = \mathbf{0} \ . \qquad (\mathbf{18})$$

Last, solving routinely (18) with respect to $\mathbf{B}$ and exposing the dependence of $\mathbf{T}(\mathbf{B})$, $\mathbf{D}(\mathbf{B})$, $\mathbf{V}(\mathbf{B})$, and $\mathbf{Z}(\mathbf{B})$ on the solution $\hat{\mathbf{B}}$ we obtain the desired BMEVA estimator

$$\hat{\mathbf{B}} = \mathbf{W}(\hat{\mathbf{B}}) [\, \mathbf{V}(\hat{\mathbf{B}}) - \mathbf{Z}(\hat{\mathbf{B}}) \,] \ , \qquad (\mathbf{19})$$

where

$$\mathbf{W}(\hat{\mathbf{B}}) = (\mathbf{T}(\hat{\mathbf{B}}) + 2\alpha \mathbf{D}^2(\hat{\mathbf{B}}) \mathbf{M} + 2\gamma \mathbf{Q})^{-1} \ , \qquad (\mathbf{20})$$

represents the adaptively regularized VA-balanced nonlinear spatial window operator. The derived BMEVA estimator (19), (20) can be converted into an efficient iterative algorithm using the Seidel fixed-point iteration method [11]. Pursuing such the approach [11], we refer to the SSP estimate on the right-hand side in (19) as the current estimate $\hat{\mathbf{B}}^{(t)}$ at the tth iteration step, and associate the entire right-hand side of (19) with the rule for forming the estimate $\hat{\mathbf{B}}^{(t+1)}$ for the next iteration step (t+1) that yields

$$\hat{\mathbf{B}}^{(t+1)} = \mathbf{W}(\hat{\mathbf{B}}^{(t)}) [\, \mathbf{V}(\hat{\mathbf{B}}^{(t)}) - \mathbf{Z}(\hat{\mathbf{B}}^{(t)}) \,] . \qquad (\mathbf{21})$$

Due to the performed regularized windowing (20), the iterative algorithm (21) converges in a polynomial time [8] regardless of the choice of the balance factor γ within the prescribed normalization interval, $0 \le \gamma \le 1$. Note, that in the

simulations reported in the next resuming section, forty iterations were sufficient to provide the 1% convergence error rate, (i.e. $\| \hat{\mathbf{B}}^{(t+1)} - \mathbf{B}^{(t)} \|^2 \leq 10^{-2} \forall t > 40$) of the developed iterative BMEVA algorithm (21) for all considered simulation scenarios.

6 Simulations and Discussions

In the simulations, we considered the SAR with partially (fractionally) synthesized aperture as an RS imaging system [6], [14]. The SFO was factorized along two axes in the image frame: the azimuth (horizontal axis) and the range (vertical axis). Following the common practically motivated technical considerations [3], [6], [14] we modeled a triangular shape of the SAR range ambiguity function (AF) of 3 pixels width of the 256-by-256 frame pixel format, and two side-looking SAR azimuth AFs for two typical scenarios of fractionally synthesized apertures: (i) azimuth AF of a Gaussian shape of 5 pixels width at 0.5 of its maximum level associated with the first system model and (ii) azimuth AF of a $|\text{sinc}|^2$ shape of 7 pixels width at the zero crossing level associated with the second system model, respectively. In the simulations, the developed BMEVA method was implemented iteratively (21) and compared with the conventional matched spatial filtering (MSF) low-resolution image formation method [2], [3] and the previously proposed high-resolution BME and VA approaches to illustrate the advantages of the fused strategy. The results of the simulation experiment indicative of the reconstruction quality are reported in Figures 1 thru 4 for two different RS scenes borrowed from the real-world RS imagery of the Metropolitan area of Guadalajara city, Mexico [16]. Figures 1.a. thru 4.a show the original super-high resolution test scenes (not observable in the simulation experiments with partially synthesized SAR system models). Figures 1.b thru 4.b present the results of SSP imaging with the conventional MSF algorithm [2]. Figures 1.c thru 4.c present the SSP frame enhanced with the VA method [7]. Figures 1.d thru 4.d show the images reconstructed with the BME method [6]. Figures 1.e thru 4.e show the images reconstructed applying the proposed BMEVA technique for the equally balanced criterions in the fused strategy, i.e. γ=1 [15]. Finally, figures 1.f thru 4.f present the BMEVA reconstruction results for experimentally adjusted balance factor γ=0.25 [15]. Finally, the quantitative performance enhancement metrics evaluated as the improvement in the output signal to noise ratio (IOSNR) [4] were calculated for the simulations with different input SNRs (μ) and the resulting IOSNRs are reported in Tables 1 and 2. The qualitative simulation results presented in Figures 1 thru 4 and corresponding quantitative performance metrics reported in Tables 1 and 2 manifest the considerably enhanced reconstruction performances achieved with the proposed BMEVA method in comparison with the previously developed BME and VA approaches that do not employ the fusion strategy.

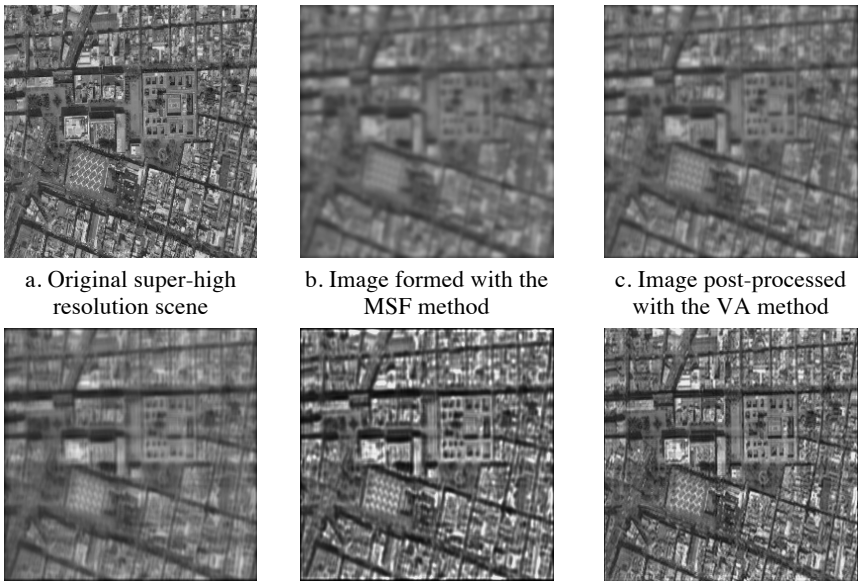

a. Original super-high resolution scene

b. Image formed with the MSF method

c. Image post-processed with the VA method

d. SSP reconstructed with the BME method

e. SSP reconstructed with the BMEVA method (γ=1)

f. SSP reconstructed with BMEVA method (γ=0.25)

Fig. 1. Simulation results for the first scene: first system model

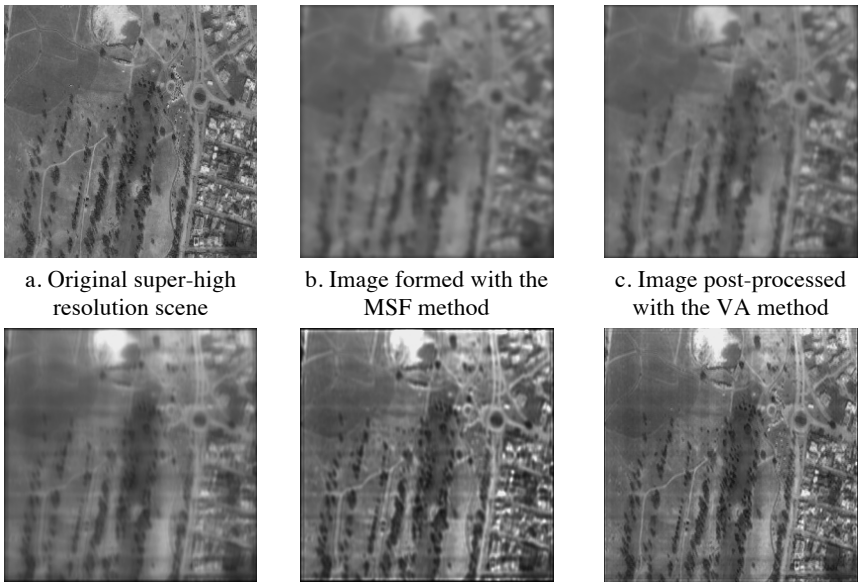

a. Original super-high resolution scene

b. Image formed with the MSF method

c. Image post-processed with the VA method

d. SSP reconstructed with the BME method

e. SSP reconstructed with the BMEVA method (γ=1)

f. SSP reconstructed with BMEVA method (γ=0.25)

Fig. 2. Simulation results for the second scene: first system model

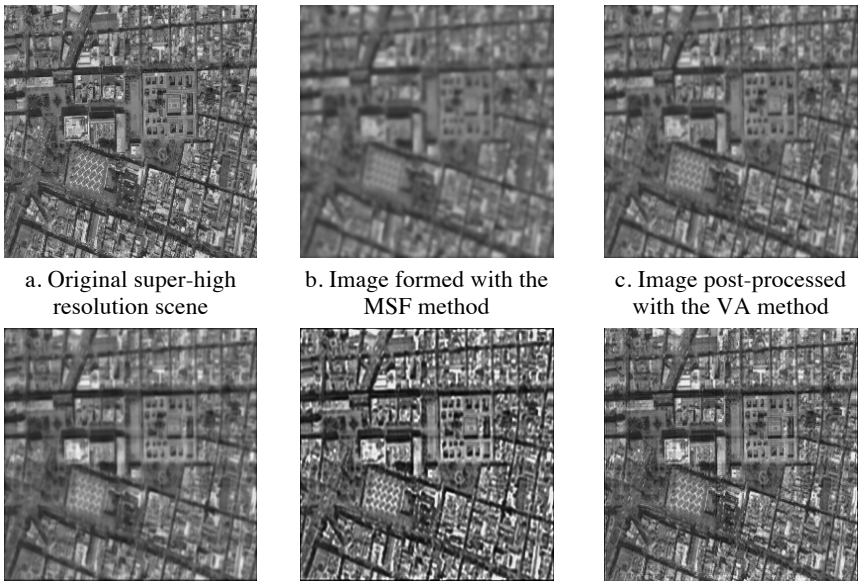

a. Original super-high resolution scene

b. Image formed with the MSF method

c. Image post-processed with the VA method

d. SSP reconstructed with the BME method

e. SSP reconstructed with the BMEVA method (γ=1)

f. SSP reconstructed with BMEVA method (γ=0.25)

Fig. 3. Simulation results for the first scene: second system model

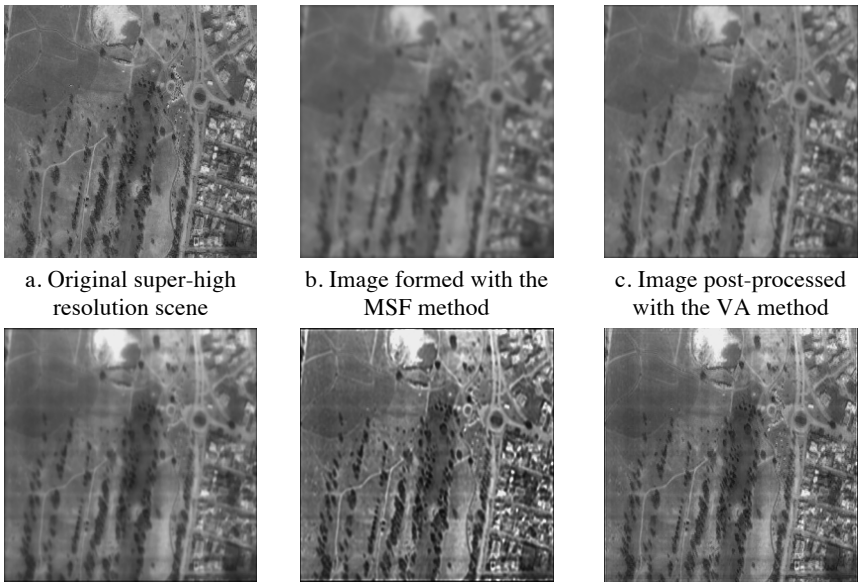

a. Original super-high resolution scene

b. Image formed with the MSF method

c. Image post-processed with the VA method

d. SSP reconstructed with the BME method

e. SSP reconstructed with the BMEVA method (γ=1)

f. SSP reconstructed with BMEVA method (γ=0.25)

Fig. 4. Simulation results for the second scene: second system model

Table 1. IOSNR values [dB] provided with different reconstruction methods. Results are reported for different SNR μ for the first test scenes and two different simulated SAR systems

SNR [dB]	*IOSNR* [dB] System 1 Reconstruction Method				*IOSNR* [dB] System 2 Reconstruction Method			
μ	*VA*	*BME*	*BMEVA* (γ=1)	*BMEVA* (γ=0.25)	*VA*	*BME*	*BMEVA* (γ=1)	*BMEVA* (γ=0.25)
10	0.811	3.671	4.551	4.898	2.012	6.208	8.581	9.021
15	0.813	3.641	4.606	4.900	2.009	6.232	8.667	9.141
20	0.812	3.629	4.673	4.906	1.999	6.264	8.628	8.968
25	0.815	3.626	4.669	4.901	2.012	6.319	8.704	8.970
30	0.813	3.627	4.643	4.912	2.011	6.350	8.739	9.067

Table 2. IOSNR values provided with different reconstruction methods. Results are reported for different SNRs for the second test scenes and two different simulated SAR systems

SNR [dB]	*IOSNR* [dB] System 1 Reconstruction Method				*IOSNR* [dB] System 2 Reconstruction Method			
μ	*VA*	*BME*	*BMEVA* (γ=1)	*BMEVA* (γ=0.25)	*VA*	*BME*	*BMEVA* (γ=1)	*BMEVA* (γ=0.25)
10	0.726	3.220	7.630	7.871	1.923	4.402	10.761	11.301
15	0.728	3.849	7.638	7.880	1.913	4.812	10.783	11.356
20	0.728	4.933	7.652	7.977	1.947	5.445	10.796	11.354
25	0.725	5.930	7.669	7.981	1.921	6.393	10.843	11.356
30	0.725	6.932	7.685	7.980	1.923	7.434	10.802	11.422

Qualitatively, the enhancement results in better detailed inhomogeneous regions with better preserved edges between the homogeneous zones. Also, the imaging artifacts typical to the reconstructions performed with the inversion techniques are considerably suppressed. The achieved enhancement effects can be explained as a result of incorporating the balanced control of the adaptive regularization with preservation of the image geometrical features performed with the BMEVA technique

7 Concluding Remarks

In summary, we may conclude that the proposed BMEVA method provides the considerably improved image reconstruction achieved due to performing the adaptive (i.e. nonlinear) regularized windowing in the flat regions with enhanced preservation of the edge features.

The new approach incorporates also some adjustable parameters viewed as the regularization degrees of freedom. Those are invoked from the BME and VA methods. The BMEVA method aggregates the image model and system-level considerations into the fused SSP reconstruction strategy providing a regularized balance between the noise suppression and gained spatial resolution with the VA-controlled geometrical properties of the resulting solution. The reported simulations demonstrate the efficiency of the developed method.

References

1. Falkovich, S.E., Ponomaryov, V.I., Shkvarko, Y.V.: Optimal Reception of Space-Time Signals in Channels with Scattering. Radio I Sviaz, Moscow (1989)
2. Wehner, D.R.: High-Resolution Radar. 2nd edn. Artech House, Boston (1994)
3. Henderson, F.M., Lewis, A.V.: Principles and Applications of Imaging Radar. In: Manual of Remote Sensing. 3rd edn. Wiley, New York (1998)
4. Shkvarko, Y.V.: Estimation of Wavefield Power Distribution in the Remotely Sensed Environment: Bayesian Maximum Entropy Approach. IEEE Transactions on Signal Processing. Vol. 50. IEEE, (2002) 2333-2346
5. Shkvarko, Y.V.: Unifying Regularization and Bayesian Estimation Methods for Enhanced Imaging with Remotely Sensed Data. Part I – Theory. IEEE Transactions on Geoscience and Remote Sensing. Vol. 42. IEEE, (2004) 923-931
6. Shkvarko, Y.V.: Unifying Regularization and Bayesian Estimation Methods for Enhanced Imaging with Remotely Sensed Data. Part II – Implementation and Performance Issues. IEEE Transactions on Geoscience and Remote Sensing. Vol. 42. IEEE, (2004) 932-940
7. Black, M., Sapiro, G., Marimont, D. H., and Hegger, D.: Robust Anisotropic Diffusion, IEEE Trans. Image Processing, Vol. 7, 3 (1998) 421-432
8. Starck, J.L., Murtagh, F., Bijaoui, A.: Image Processing and Data Analysis: The Multiscale Approach. Cambridge University Press, Cambridge (1998)
9. Ben Hamza, A., Krim, H., B. Unal, G.: Unifying Probabilistic and Variational Estimation. IEEE Signal Processing Magazine, Vol. 19, (2002) 37-47
10. John, S., Vorontsov M.: Multiframe Selective Information Fusion From Robust Error Estimation Theory, IEEE Trans. Image Processing, Vol. 14, 5 (2005) 577-584
11. Barrett, H.H., Myers, K.J.: Foundations of Image Science. Wiley, New York (2004)
12. Vazquez-Bautista, R.F., Morales-Mendoza, L.J., and Shkvarko, Y.V.: Aggregating the Statistical Estimation and Variational Analysis Methods in Radar Imagery. IEEE International Geoscience and Remote Sensing Symposium, IGARSS. Vol. 3. Toulouse, France (2003) 2008 – 2010
13. Erdogmus, D., Principe, J.C.: From Linear Adaptive Filtering to Nonlinear Information Processing. IEEE Signal Processing Magazine. Vol. 23. IEEE, (2006) 14-33
14. Franceschetti, G., Iodice, A., Perna, S., Riccio, D.: Efficient Simulation of Airborne SAR Raw Data of Extended Scenes. IEEE Transactions on Geoscience and Remote Sensing. Vol. 44. IEEE, (2006) 2851-2860
15. Morales-Mendoza, L.J., Vazquez-Bautista, R.F., and Shkvarko, Y.V.: Unifying the Maximum Entropy and Variational Analysis Regularization Methods for Reconstruction of the Remote Sensing Imagery. IEEE Latin America Transactions. Vol. 3. IEEE, (2005) 60-73

16. Space Imaging. In: http://www.spaceimaging.com/quicklook. GeoEye Inc., (2007)